EUROPEAN ORGANIZATION FOR NUCLEAR RESEARCH (CERN)

Observation of new resonances decaying to $J/\psi K^+$ and $J/\psi\phi$

LHCb collaboration[†]

Abstract

The first observation of exotic states with a new quark content $c\bar{c}u\bar{s}$ decaying to the $J/\psi K^+$ final state is reported with high significance from an amplitude analysis of the $B^+ \to J/\psi\phi K^+$ decay. The analysis is carried out using proton-proton collision data corresponding to a total integrated luminosity of $9\,\text{fb}^{-1}$ collected by the LHCb experiment at centre-of-mass energies of 7, 8 and 13 TeV. The most significant state, $Z_{cs}(4000)^+$, has a mass of $4003 \pm 6\,{}^{+\,4}_{-\,14}\,\text{MeV}$, a width of $131 \pm 15 \pm 26\,\text{MeV}$, and spin-parity $J^P = 1^+$, where the quoted uncertainties are statistical and systematic, respectively. A new 1^+ $X(4685)$ state decaying to the $J/\psi\phi$ final state is also observed with high significance. In addition, the four previously reported $J/\psi\phi$ states are confirmed and two more exotic states, $Z_{cs}(4220)^+$ and $X(4630)$, are observed with significance exceeding five standard deviations.

[†]Authors are listed at the end of this paper.

Since the discovery of the $X(3872)$ state by the Belle experiment in 2003 [1], more than twenty non-conventional hadrons that contain $c\bar{c}$ or $b\bar{b}$ quarks have been uncovered [2]. In contrast to the neutral states, charged states like $Z_c(3900)^+$ [3, 4] and $Z_c(4430)^+$ [5–7] provide evidence for tetraquark exotic states, because light quarks are required to account for the non-zero electric charge in addition to the heavy quarkonium.[1] Previously, only the u or d quarks were observed to constitute the light quark content of such charged exotic states, even though the existence of a Z_{cs} state as a strangeness-flavour partner of the $Z_c^+(3900)$ state has been predicted [8–12]. Recently, the BESIII experiment reported a 5.3 standard deviation (σ hereafter) observation of a threshold structure in the mass distribution of $D_s^- D^{*0} + D_s^{*-} D^0$ pairs produced in e^+e^- annihilation as recoil against a K^+ meson [13].

In this Letter, the first observation of two charged $Z_{cs}^+ \rightarrow J/\psi K^+$ states is reported from an updated amplitude analysis of the $B^+ \rightarrow J/\psi \phi K^+$ decay, as well as the observation of two more $X \rightarrow J/\psi \phi$ states. The analysis is based on the combined proton-proton (pp) collision data collected using the LHCb detector in Run 1 at centre-of-mass energies $\sqrt{s}$ of 7 and 8 TeV, corresponding to a total integrated luminosity of $3\,\mathrm{fb}^{-1}$, and in Run 2 at $\sqrt{s} = 13\,\mathrm{TeV}$ corresponding to an integrated luminosity of $6\,\mathrm{fb}^{-1}$.

With Run 1 data, LHCb performed the first amplitude analysis of the $B^+ \rightarrow J/\psi \phi K^+$ decay, investigating the $J/\psi \phi$ structure [14,15] in addition to the kaon excitations (hereafter indicated as K^{*+}). The decay amplitude was constructed using the helicity formalism in six dimensions which, in addition to the Dalitz plane variables describing the $B^+ \rightarrow J/\psi \phi K^+$ decay, made use of the $J/\psi \rightarrow \mu^+ \mu^-$ and the $\phi \rightarrow K^+ K^-$ decay angles, providing the best sensitivity to the contributing resonances and the determination of their quantum numbers. Resonance lineshapes were parametrised using the Breit-Wigner approximation. The data were described with seven $K^{*+} \rightarrow \phi K^+$ resonances, four $X \rightarrow J/\psi \phi$ structures, and non-resonant (NR) ϕK^+ and $J/\psi \phi$ contributions. The four X structures and the NR $J/\psi \phi$ contribution were observed with significance above 5σ. The existence of the $X(4274)$ state was established. The J^{PC} quantum numbers of the $X(4140)$ and $X(4274)$ states were determined as 1^{++} above 5σ level, and as 0^{++} for the $X(4500)$ and $X(4700)$ states above 4σ (the recent PDG convention labels these states as χ_{cJ} [2]). Notably, the $X(4140)$ width was substantially larger than previously determined [16–18]. In the Run 1 analysis, $Z_{cs}^+ \rightarrow J/\psi K^+$ contributions were also tested [14,15]. Around a 3σ evidence for a Z_{cs}^+ state was found, but deemed insufficient to claim discovery of an exotic state with a new quark content.

The LHCb detector is a single-arm forward spectrometer covering the pseudorapidity range $2 < \eta < 5$, described in detail in Refs. [19,20]. Simulation is produced with software packages described in Refs. [21–24]. The $B^+ \rightarrow J/\psi(\rightarrow \mu^+\mu^-)\phi(\rightarrow K^+K^-)K^+$ signal candidates are first required to pass an online event selection performed by a trigger [25] dedicated for selecting J/ψ candidates. The signal decay is reconstructed by combining the J/ψ candidate with three kaon candidates with a total charge of one unit. The ϕ candidate is selected by requiring only one of two K^+K^- combinations to be consistent with the known ϕ mass [2] within $\pm 15\,\mathrm{MeV}$.[2]

The offline selection involves a loose preselection, followed by a multivariate classifier based on a Gradient Boosted Decision Tree (BDTG) [26,27]. The preselection is similar to

---

[1]Charge conjugation is implied throughout this Letter.
[2]Natural units with $\hbar = c = 1$ are used throughout.
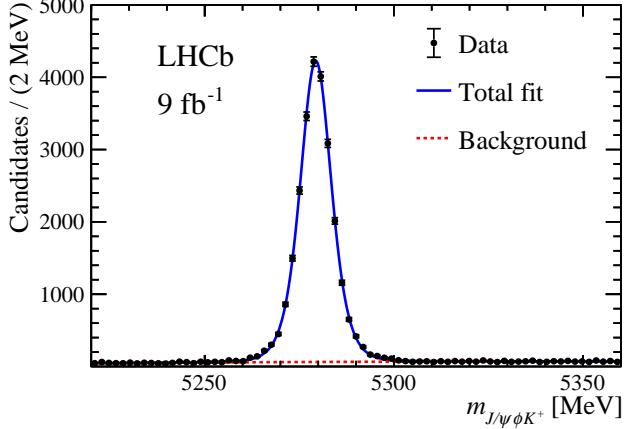
Figure 1: Invariant-mass distribution of selected $B^+ \to J/\psi\phi K^+$ candidates with the fit overlaid.

that used in Refs. [14, 15] but the requirement on the χ^2_{IP} of kaon candidates is loosened, where χ^2_{IP} is defined as the difference in the vertex-fit χ^2 of the event primary pp collision vertex (PV) candidate, reconstructed with and without the particle considered. The BDTG response is constructed using eight variables: the kaon minimum χ^2_{IP}, the minimum kaon particle identification probability, and the scalar sum of kaon momentum component transverse to the beam direction (p_{T}), the B^+ candidate p_{T}, its decay vertex-fix quality, the B^+ χ^2_{IP}, the χ^2 of the flight distance with respect to the associated PV, and the angle between the reconstructed momentum direction and the vector connecting the associated PV and the B^+ decay vertex, where the associated PV is the one that gives the smallest χ^2_{IP} among all PVs. The BDTG is trained on simulated $B^+ \to J/\psi\phi K^+$ decays generated uniformly in phase space for the signal sample, and data from the B^+ candidate invariant mass sidebands for the background sample. The requirement on the BDTG response is chosen to maximise the signal significance multiplied by the purity [28].

A kinematic fit [29] is applied to the reconstructed $B^+ \to J/\psi\phi K^+$ decay to improve the mass resolution, where the J/ψ candidate mass is constrained to its known value [2] and the B^+ candidate is constrained to originate from the associated PV. The resulting invariant-mass distribution of the B^+ candidates is shown in Fig. 1, fitted with the signal modelled by a Hypatia function [30] and the combinatorial background by a second-order polynomial function, yielding $24\,220 \pm 170$ signal candidates with a combinatorial-background fraction of 4.0% within a $\pm 15\,\mathrm{MeV}$ signal region. The region also includes additional $\sim 2\%$ of non-ϕ $B^+ \to J/\psi K^+ K^- K^+$ background candidates, which are neglected in the amplitude model but considered in the evaluation of the systematic uncertainties. The candidates in the signal region are retained for further amplitude analysis. Compared to the previous Run 1 analysis [14, 15], the total signal yield is ~ 6 times larger, owing to a larger dataset and a 15% higher signal efficiency. The fraction of combinatorial background is almost a factor of six smaller while that of the non-ϕ background is unchanged.

A second kinematic fit is performed to improve the momentum resolution of the final-state particles by further constraining the $J/\psi\phi K^+$ candidate mass to the known B^+ mass value [2]. The updated particle momenta are used to calculate the fit observables in the amplitude analysis. Fig. 2 shows the Dalitz plots for candidates in the B^+ signal region. The most apparent features are four bands in the $J/\psi\phi$ mass distribution, corresponding

2
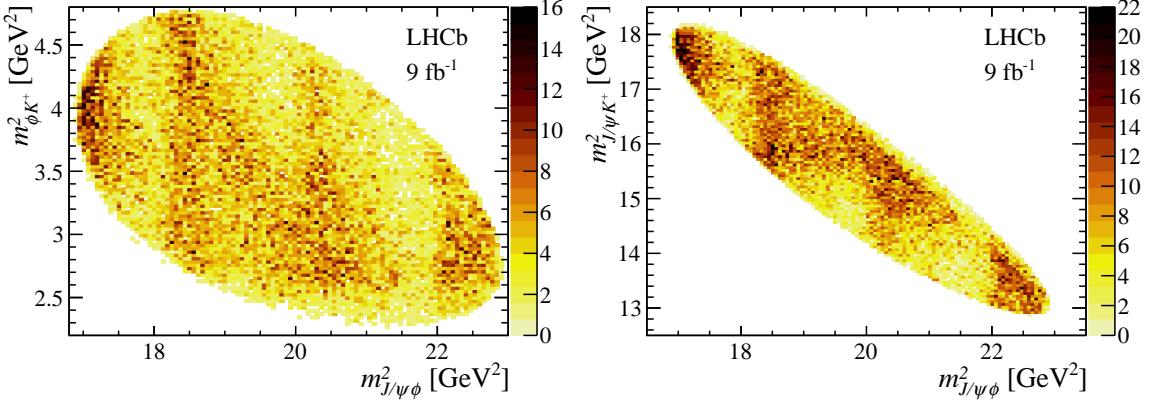
Figure 2: Dalitz plots for $B^+ \to J/\psi\phi K^+$ candidates in a region $\pm 15\,\mathrm{MeV}$ around the B^+ mass peak.

to the previously reported $X(4140)$, $X(4274)$, $X(4500)$ and $X(4700)$ states. There is also a distinct band near $16\,\mathrm{GeV}^2$ of the $J/\psi K^+$ mass squared.

To investigate the resonant structures, a full amplitude fit is performed using an unbinned maximum-likelihood method. The likelihood definition and the total probability density function (PDF), which includes a signal and a background component, are described in the previous publication [15]. The signal B^+ decay is described in the helicity formalism by three decay chains: $K^{*+}(\to \phi K^+)J/\psi$, $X(\to J/\psi\phi)K^+$ and $Z_{cs}^+(\to J/\psi K^+)\phi$. Each chain is fully described by one mass and five angular observables. For example, the conventional K^{*+} chain has the following six observables $\Phi \equiv (m_{\phi K}, \theta_{K^*}, \theta_{J/\psi}, \theta_\phi, \Delta\varphi_{K^*,J/\psi}, \Delta\varphi_{K^*,\phi})$, where θ denotes the helicity angles, and $\Delta\varphi$ the angles between two decay planes. Due to the non-scalar final-state particles (μ^+ and μ^-), an azimuthal angle α_μ^i is required to align the helicity frames of μ^+ and μ^- between the chain i and the reference K^{*+} chain [6, 7, 31].

The model used in the previous study (Run 1 model) is first tested. Due to the increased sample size, the model requires improvements (see Fig. 3 bottom row). To improve the K^{*+} model, the tails of the $K^*(1410)$, $K(1460)$, and $K_1(1400)$ resonances with poles just below the ϕK^+ mass threshold are included. The tail of the $K_1(1400)$ leads to a better description of the data than the $J^P = 1^+$ NR component previously used, as well as the introduction of the 0^- $K(1460)$ contribution describes the data better than the previously used but insignificant state at $1.8\,\mathrm{GeV}$. Nine K^{*+} states are included in the default model as listed in Table 1. Seven more K^{*+} states predicted in the allowed ϕK^+ mass range by the relativistic potential model by Godfrey-Isgur [32] are tested, but since these components are not above 5σ significance, they are considered only in the systematic studies. At the next step, X or Z_{cs}^+ states of different J^P hypotheses are tested in the fit one at a time. The two states (1^+ Z_{cs}^+ and 1^+ X) which produce the largest likelihood improvements are included first. In the second iteration, several other states produce large fit improvements, a Z_{cs}^+ state (either 1^+ or 1^-), and two X states with 1^- and 2^-, are also included in the default model. In total, nine K^{*+}, seven X, two Z_{cs}^+, and one $J/\psi\phi$ NR component, including three new X and two Z_{cs}^+ components, are taken as the default model. All of these components have a statistical significance above 5σ, as evaluated by taking them out of the model one at a time. No further components are found which satisfy this criterion.

3

Table 1: Fit results from the default amplitude model. The significances are evaluated accounting for total (statistical) uncertainties. The listed masses and widths without uncertainties are taken from PDG [2] and are fixed in the fit. The listed world averages of the two K_2 and $K^*(1680)$ resonances do not contain the contributions from the previous LHCb Run 1 results.

|	Contribution	Significance [×σ]	M_0 [MeV]	Γ_0 [MeV]	FF [%]
	All $K(1^+)$				$25 \pm 4\,^{+\,6}_{-15}$
2^1P_1	$K(1^+)$	4.5 (4.5)	$1861 \pm 10\,^{+\,16}_{-\,46}$	$149 \pm 41\,^{+231}_{-\,23}$	
2^3P_1	$K'(1^+)$	4.5 (4.5)	$1911 \pm 37\,^{+124}_{-\,48}$	$276 \pm 50\,^{+319}_{-159}$	
1^3P_1	$K_1(1400)$	9.2 (11)	1403	174	$15 \pm 3\,^{+\,3}_{-11}$
	All $K(2^-)$				$2.1 \pm 0.4\,^{+2.0}_{-1.1}$
1^1D_2	$K_2(1770)$	7.9 (8.0)	1773	186	
1^3D_2	$K_2(1820)$	5.8 (5.8)	1816	276	
	All $K(1^-)$				$50 \pm 4\,^{+10}_{-19}$
1^3D_1	$K^*(1680)$	4.7 (13)	1717	322	$14 \pm 2\,^{+35}_{-\,8}$
2^3S_1	$K^*(1410)$	7.7 (15)	1414	232	$38 \pm 5\,^{+11}_{-17}$
	$K(2^+)$				
2^3P_2	$K_2^*(1980)$	1.6 (7.4)	$1988 \pm 22\,^{+194}_{-\,31}$	$318 \pm 82\,^{+481}_{-101}$	$2.3 \pm 0.5 \pm 0.7$
	$K(0^-)$				
2^1S_0	$K(1460)$	12 (13)	1483	336	$10.2 \pm 1.2\,^{+1.0}_{-3.8}$
	$X(2^-)$				
	$X(4150)$	4.8 (8.7)	$4146 \pm 18 \pm 33$	$135 \pm 28\,^{+59}_{-30}$	$2.0 \pm 0.5\,^{+0.8}_{-1.0}$
	$X(1^-)$				
	$X(4630)$	5.5 (5.7)	$4626 \pm 16\,^{+\,18}_{-110}$	$174 \pm 27\,^{+134}_{-\,73}$	$2.6 \pm 0.5\,^{+2.9}_{-1.5}$
	All $X(0^+)$				$20 \pm 5\,^{+14}_{-\,7}$
	$X(4500)$	20 (20)	$4474 \pm 3 \pm 3$	$77 \pm 6\,^{+10}_{-\,8}$	$5.6 \pm 0.7\,^{+2.4}_{-0.6}$
	$X(4700)$	17 (18)	$4694 \pm 4\,^{+16}_{-\,3}$	$87 \pm 8\,^{+16}_{-\,6}$	$8.9 \pm 1.2\,^{+4.9}_{-1.4}$
	$\mathrm{NR}_{J/\psi\phi}$	4.8 (5.7)			$28 \pm 8\,^{+19}_{-11}$
	All $X(1^+)$				$26 \pm 3\,^{+\,8}_{-10}$
	$X(4140)$	13 (16)	$4118 \pm 11\,^{+19}_{-36}$	$162 \pm 21\,^{+24}_{-49}$	$17 \pm 3\,^{+19}_{-\,6}$
	$X(4274)$	18 (18)	$4294 \pm 4\,^{+3}_{-6}$	$53 \pm 5 \pm 5$	$2.8 \pm 0.5\,^{+0.8}_{-0.4}$
	$X(4685)$	15 (15)	$4684 \pm 7\,^{+13}_{-16}$	$126 \pm 15\,^{+37}_{-41}$	$7.2 \pm 1.0\,^{+4.0}_{-2.0}$
	All $Z_{cs}(1^+)$				$25 \pm 5\,^{+11}_{-12}$
	$Z_{cs}(4000)$	15 (16)	$4003 \pm 6\,^{+\,4}_{-14}$	$131 \pm 15 \pm 26$	$9.4 \pm 2.1 \pm 3.4$
	$Z_{cs}(4220)$	5.9 (8.4)	$4216 \pm 24\,^{+43}_{-30}$	$233 \pm 52\,^{+97}_{-73}$	$10 \pm 4\,^{+10}_{-\,7}$
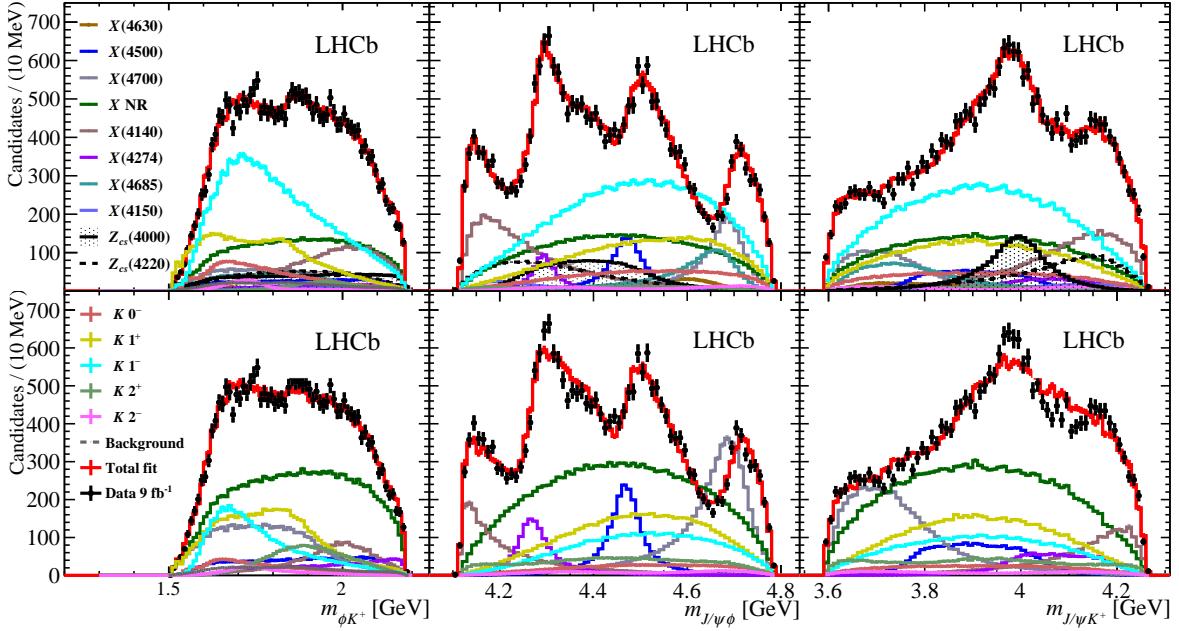
Figure 3: Distributions of ϕK^+ (left), $J/\psi\phi$ (middle) and $J/\psi K^+$ (right) invariant masses for the $B^+ \to J/\psi\phi K^+$ candidates (black data points) compared with the fit results (red solid lines) of the default model (top row) and the Run 1 model (bottom row).
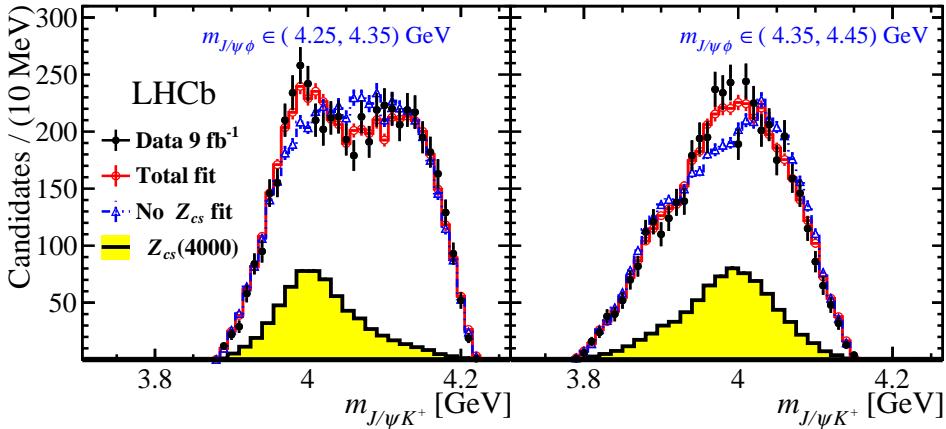

Figure 4: Fit projections onto $m_{J/\psi K^+}$ in two slices of $m_{J/\psi\phi}$ for the default model with and without the 1^+ Z_{cs}^+ states. The narrow Z_{cs}^+ state at 4 GeV is evident.

Fig. 3 shows the invariant mass distributions for all pairs of final state particles of the $B^+ \to J/\psi\phi K^+$ decay with fit projections from the amplitude analysis overlaid, for both the default model and the Run 1 model. The fit results are summarised in Table 1, including mass, width, fit fraction (FF), and significance of each component. The masses and widths of the four X states studied using the LHCb Run 1 sample only are consistent with the previous measurements [14, 15]. The significance of each component is evaluated by assuming that the change of twice the log-likelihood between the default fit and the fit without this component follows a χ^2 distribution. The corresponding number of degrees of freedom is equal to the reduction in the number of free parameters multiplied by a factor

of two (one) when the mass and width of the component are floated (fixed) in the fit, which accounts for the look-elsewhere effect [15,33], as validated by pseudoexperiments. Fig. 4 shows the $m_{J/\psi K^+}$ distributions in two slices of $m_{J/\psi\phi}$, which demonstrate the need for the narrower $Z_{cs}(4000)^+$ state. Including the 1^+ Z_{cs}^+ states improves the χ^2/nbin from 84/35 to 43/35 (left slice), and from 79/37 to 32/37 (right slice), where nbin is the number of non-zero bins.

The spin and parity of each exotic state is probed by testing alternative J^P hypotheses and comparing the fit likelihood values [15]. The J^P assignments for the previously reported four X states are confirmed with high significance. A 1^+ assignment is favoured for the new $X(4685)$ state with also high significance, but the quantum numbers of the $X(4150)$ and $X(4630)$ are less well determined. The best hypothesis for the $X(4630)$ state is 1^- over 2^- at a 3σ level. The other hypotheses are ruled out by more than 5σ. The fit prefers 2^- for the $X(4150)$ state by more than 4σ. The narrower $Z_{cs}(4000)^+$ state is determined to be 1^+ with high significance. The broader $Z_{cs}(4220)^+$ state could be 1^+ or 1^-, with a 2σ difference in favour of the first hypothesis. Other spin-parity assignments are ruled out at 4.9σ level.

Systematic uncertainties are estimated for the masses, widths, and fit fractions of the exotic states, as well as for those K^{*+} states with mass and width being free parameters in the default amplitude model. To probe the effects from the neglected non-ϕ contributions, the ϕ mass window is changed from $\pm 15\,\text{MeV}$ to $\pm 7\,\text{MeV}$, and alternatively this background is subtracted using the *sPlot* technique [34]. The Blatt-Weisskopf barrier [15] hadron size is varied between 1.5 and $4.5\,\text{GeV}^{-1}$. The default NR 0^+ $J/\psi\phi$ representation is changed from a constant to a linear polynomial, multiplied by the Blatt-Weisskopf barrier factors. Optional 1^+ or 2^+ NR $J/\psi\phi$ contributions are also included. The smallest allowed orbital angular momentum in the resonance function is varied. For the $X(4140)$, which peaks near the $J/\psi\phi$ threshold, the Flatté model [35] is used instead of the Breit-Wigner amplitude. A simplified one-channel K-matrix model [2] is used to describe various K^* resonances instead of the sum of Breit-Wigner amplitudes. Two-channel K-matrix models have also been tried for the 2^1P_1 and 2^3P_1 K^* states with the coupled-channel thresholds opening up near $1.75\,\text{GeV}$, with an insignificant improvement to the description of the $m_{\phi K}$ distribution. An extended model is tested by adding five more K^{*+} resonances, which are predicted in the allowed ϕK^+ mass range. The presence of an extra X state contribution, with J from 0 to 2, to the extended model is also checked. The difference between the results obtained from assigning 1^+ or 1^- hypotheses to the $Z_{cs}(4220)^+$ is taken as a systematic uncertainty. The mass-dependent width in the denominator of the Breit-Wigner function for the K^{*+} resonances is calculated with the lightest allowed channel (πK for natural spin-parity resonances and ωK for others) instead of ϕK.

The maximum deviation among the modelling uncertainties discussed above is summed in quadrature with the additional sources listed below. The uncertainties due to the fixed masses and widths of the known K^{*+} resonances are estimated by varying them within their known uncertainties [2]. To probe the effect of mismodelling the χ^2_{IP} of the B^+ candidate, this quantity is smeared such that the simulated distribution matches the one in the data. The uncertainty in the combinatorial background fraction is estimated by varying the background shape in the B^+ mass fit. The uncertainty in the background PDF model is estimated by using either the low or high B^+ mass sideband instead of both. The effect due to the finite size of the simulation samples is estimated using a bootstrap method [36]. For the $Z_{cs}(4000)^+$ state, the largest systematic contribution is
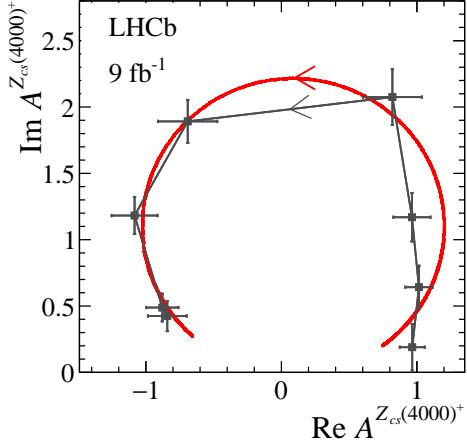
Figure 5: Fitted values of the $Z_{cs}(4000)^+$ amplitude in eight $m_{J/\psi K^+}$ intervals, shown on an Argand diagram (black points). The red curve represents the expected Breit-Wigner behaviour between $-1.4\Gamma_0$ to $1.4\Gamma_0$ around the $Z_{cs}(4000)^+$ mass.

due to the J^P hypotheses of the $Z_{cs}(4220)^+$ state. The summary of fit results, including the systematic uncertainties, is listed in Table 1. The smallest significance found when varying each of sources is taken as the significance accounting for systematic uncertainty.

Further evidence for the resonant character of $Z_{cs}(4000)^+$ is observed in Fig. 5, showing the evolution of the complex amplitude on the Argand diagram, obtained with the same method as previously reported for the $Z_c(4430)^-$ state [7]. The magnitude and phase have approximately circular evolution with $m_{J/\psi K^+}$ in the counter-clockwise direction, as expected for a resonance.

The BESIII experiment reported observation of the threshold structure in the $D_s^- D^{*0} + D_s^{*-} D^0$ mass distribution [13]. When interpreted as a resonance, called $Z_{cs}(3985)^-$, its mass $3982.5 \,^{+1.8}_{-2.6}\,(\text{stat}) \pm 2.1\,(\text{syst})$ MeV is consistent with the 1^+ $Z_{cs}(4000)^+$ state observed in this analysis, but with significantly narrower width $12.8 \,^{+5.3}_{-4.4}\,(\text{stat}) \pm 3.0\,(\text{syst})$ MeV. When fixing the mass and width of this state to the nominal BESIII result in the amplitude fit to our data, the twice the log-likelihood is worse by 160 units. The narrower width is also not supported by an alternative Flatté model with parameters obtained from our data. Therefore, there is no evidence that the $Z_{cs}(4000)^+$ state observed here is as same as the $Z_{cs}(3985)^-$ state observed by BESIII.

In conclusion, an improved full amplitude analysis of the $B^+ \to J/\psi \phi K^+$ decay is performed using 6 times larger signal yield than previously analyzed [14]. A relatively narrow $Z_{cs}(4000)^+$ state decaying to $J/\psi K^+$ with mass $4003 \pm 6\,(\text{stat})\,^{+4}_{-14}\,(\text{syst})$ MeV and width $131 \pm 15\,(\text{stat}) \pm 26\,(\text{syst})$ MeV is observed with large significance. Its spin-parity is determined to be 1^+ also with high significance. A quasi-model-independent representation of the $Z_{cs}(4000)^+$ contribution in the fit shows a phase change in the amplitude consistent with that of a resonance. A broader 1^+ or 1^- $Z_{cs}(4220)^+$ state is also required at 5.9σ. This is the first observation of states with hidden charm and strangeness that decay to the $J/\psi K^+$ final state. The four X states decaying to $J/\psi \phi$ observed in the Run 1 analysis [14] are confirmed with higher significance, together with their quantum number assignments. An additional 1^+ $X(4685)$ state is observed with relatively narrow width (about 125 MeV) with high significance. A new $X(4630)$ state is observed with a 5.5σ significance, with

preferred 1^- over 2^- spin-parity assignment at 3σ level, and the other J^P hypotheses rejected at 5σ. This constitutes the first observation of exotic states with a new quark content $c\bar{c}u\bar{s}$ decaying to the $J/\psi K^+$ final state.

Acknowledgements

References

[1] Belle collaboration, S. K. Choi *et al.*, *Observation of a narrow charmonium - like state in exclusive $B^\pm \to K^\pm \pi^+ \pi^- J/\psi$ decays*, Phys. Rev. Lett. **91** (2003) 262001, `arXiv:hep-ex/0309032`.

[2] Particle Data Group, P. A. Zyla *et al.*, *Review of particle physics*, Prog. Theor. Exp. Phys. **6** (2020) 083C01.

[3] BESIII collaboration, M. Ablikim *et al.*, *Observation of a charged charmoniumlike structure in $e^+e^- \to \pi^+\pi^- J/\psi$ at $\sqrt{s} = 4.26\ GeV$*, Phys. Rev. Lett. **110** (2013) 252001, `arXiv:1303.5949`.

[4] Belle collaboration, Z. Q. Liu *et al.*, *Study of $e^+e^- \to \pi^+\pi^- J/\psi$ and observation of a charged charmoniumlike state at Belle*, Phys. Rev. Lett. **110** (2013) 252002, `arXiv:1304.0121`.

[5] Belle collaboration, S. K. Choi *et al.*, *Observation of a resonance-like structure in the $\pi^\pm \psi'$ mass distribution in exclusive $B \to K \pi^\pm \psi'$ decays*, Phys. Rev. Lett. **100** (2008) 142001, `arXiv:0708.1790`.

[6] Belle collaboration, K. Chilikin *et al.*, *Experimental constraints on the spin and parity of the $Z(4430)^+$*, Phys. Rev. **D88** (2013) 074026, `arXiv:1306.4894`.

[7] LHCb collaboration, R. Aaij *et al.*, *Observation of the resonant character of the $Z(4430)^-$ state*, Phys. Rev. Lett. **112** (2014) 222002, `arXiv:1404.1903`.

[8] M. B. Voloshin, *Strange hadrocharmonium*, Phys. Lett. **B798** (2019) 135022, `arXiv:1901.01936`.

[9] J. M. Dias, X. Liu, and M. Nielsen, *Prediction for the decay width of a charged state near the $D_s\bar{D}^*/D_s^*\bar{D}$ threshold*, Phys. Rev. **D88** (2013) 096014, `arXiv:1307.7100`.

[10] D.-Y. Chen, X. Liu, and T. Matsuki, *Predictions of charged charmoniumlike structures with hidden-charm and open-strange channels*, Phys. Rev. Lett. **110** (2013) 232001, `arXiv:1303.6842`.

[11] J. Ferretti and E. Santopinto, *Hidden-charm and bottom tetra- and pentaquarks with strangeness in the hadro-quarkonium and compact tetraquark models*, JHEP **04** (2020) 119, `arXiv:2001.01067`.

[12] S. H. Lee, M. Nielsen, and U. Wiedner, *D(s)D* molecule as an axial meson*, J. Korean Phys. Soc. **55** (2009) 424, `arXiv:0803.1168`.

[13] BESIII collaboration, M. Ablikim *et al.*, *Observation of a near-threshold structure in the K^+ recoil-mass spectra in $e^+e^- \to K^+(D_s^-D^{*0} + D_s^{*-}D^0)$*, `arXiv:2011.07855`.

[14] LHCb collaboration, R. Aaij *et al.*, *Observation of exotic $J/\psi\phi$ structures from amplitude analysis of $B^+ \to J/\psi\phi K^+$ decays*, Phys. Rev. Lett. **118** (2017) 022003, `arXiv:1606.07895`.

[15] LHCb collaboration, R. Aaij *et al.*, *Amplitude analysis of $B^+ \to J/\psi\phi K^+$ decays*, Phys. Rev. **D95** (2017) 012002, `arXiv:1606.07898`.

[16] CDF collaboration, T. Aaltonen *et al.*, *Evidence for a narrow near-threshold structure in the $J/\psi\phi$ mass spectrum in $B^+ \to J/\psi\phi K^+$ decays*, Phys. Rev. Lett. **102** (2009) 242002, `arXiv:0903.2229`.

[17] CDF, T. Aaltonen *et al.*, *Observation of the $Y(4140)$ structure in the $J/\psi\phi$ mass spectrum in $B^\pm \to J/\psi\phi K^\pm$ decays*, Mod. Phys. Lett. A **32** (2017) 1750139, `arXiv:1101.6058`.

[18] CMS collaboration, S. Chatrchyan *et al.*, *Observation of a peaking structure in the $J/\psi\phi$ mass spectrum from $B^\pm \to J/\psi\phi K^\pm$ decays*, Phys. Lett. **B734** (2014) 261, `arXiv:1309.6920`.

[19] LHCb collaboration, A. A. Alves Jr. *et al.*, *The LHCb detector at the LHC*, JINST **3** (2008) S08005.

[20] LHCb collaboration, R. Aaij *et al.*, *LHCb detector performance*, Int. J. Mod. Phys. **A30** (2015) 1530022, `arXiv:1412.6352`.

[21] T. Sjöstrand, S. Mrenna, and P. Skands, *A brief introduction to PYTHIA 8.1*, Comput. Phys. Commun. **178** (2008) 852, arXiv:0710.3820.

[22] I. Belyaev *et al.*, *Handling of the generation of primary events in Gauss, the LHCb simulation framework*, J. Phys. Conf. Ser. **331** (2011) 032047.

[23] D. J. Lange, *The EvtGen particle decay simulation package*, Nucl. Instrum. Meth. **A462** (2001) 152.

[24] Geant4 collaboration, J. Allison *et al.*, *Geant4 developments and applications*, IEEE Trans. Nucl. Sci. **53** (2006) 270; Geant4 collaboration, S. Agostinelli *et al.*, *Geant4: A simulation toolkit*, Nucl. Instrum. Meth. **A506** (2003) 250.

[25] R. Aaij *et al.*, *The LHCb trigger and its performance in 2011*, JINST **8** (2013) P04022, arXiv:1211.3055.

[26] L. Breiman, J. H. Friedman, R. A. Olshen, and C. J. Stone, *Classification and regression trees*, Wadsworth international group, Belmont, California, USA, 1984; H. Voss, A. Hoecker, J. Stelzer, and F. Tegenfeldt, *TMVA - Toolkit for Multivariate Data Analysis with ROOT*, PoS **ACAT** (2007) 040.

[27] A. Hoecker *et al.*, *TMVA 4 — Toolkit for Multivariate Data Analysis with ROOT. Users Guide.*, arXiv:physics/0703039.

[28] LHCb collaboration, R. Aaij *et al.*, *Amplitude analysis of $B_s^0 \to K_S^0 K^{\pm} \pi^{\mp}$ decays*, JHEP **06** (2019) 114, arXiv:1902.07955.

[29] W. D. Hulsbergen, *Decay chain fitting with a Kalman filter*, Nucl. Instrum. Meth. **A552** (2005) 566, arXiv:physics/0503191.

[30] D. Martínez Santos and F. Dupertuis, *Mass distributions marginalized over per-event errors*, Nucl. Instrum. Meth. **A764** (2014) 150, arXiv:1312.5000.

[31] Belle collaboration, R. Mizuk *et al.*, *Observation of two resonance-like structures in the $\pi^+ \chi_{c1}$ mass distribution in exclusive $\bar{B}^0 \to K^- \pi^+ \chi_{c1}$ decays*, Phys. Rev. **D78** (2008) 072004, arXiv:0806.4098.

[32] S. Godfrey and N. Isgur, *Mesons in a relativized quark model with chromodynamics*, Phys. Rev. **D32** (1985) 189.

[33] L. Lyons, *Open statistical issues in Particle Physics*, Ann. Appl. Stat. **2** (2008) 887, arXiv:0811.1663.

[34] M. Pivk and F. R. Le Diberder, *sPlot: A statistical tool to unfold data distributions*, Nucl. Instrum. Meth. **A555** (2005) 356, arXiv:physics/0402083.

[35] S. M. Flatté, *Coupled-channel analysis of the $\pi\eta$ and $K\overline{K}$ systems near $K\overline{K}$ threshold*, Phys. Lett. **B63** (1976) 224.

[36] B. Efron, *Bootstrap methods: another look at the jackknife*, Annals Statist. **7** (1979) 1.

PRL justification

Exotic states, with quark configurations other than three quarks or quark-antiquark, can reveal new or hidden aspects of the dynamics of the strong interactions. An improved full amplitude analysis of $B^+ \to J/\psi\phi K^+$ decays is performed using 6 times larger signal yield than previously analyzed. We report the first observation of two exotic states with a new quark content $c\bar{c}u\bar{s}$ decaying to the $J/\psi K^+$ final state. Two new $X \to J/\psi\phi$ states are also observed with high significance. Four X states previously observed by LHCb are also confirmed.

Word Count

main-count contains 18213 characters and 2968 words. Figures: Add 20+150/(aspect ratio) per figure:

20+150/1.5 + 20+150/2 + 20+150/(2./3.) + 20+150/2 + 20 + 150/1.5 = 675

Equations: Add 16 words per row (single column): 0

Tables: Add 13 words plus 6.5 words per line (single column) : 13+6.5*31=214.5

In total there are 3857.5 words.

Supplementary material for LHCb-PAPER-2020-044

This appendix contains supplementary material that will be posted on the public CDS record but will not appear in the paper.

1 Angular moments

The unnormalized Legendre moments are defined as

$$< P_\ell^U >= \sum_{i=1}^{N_{\text{events}}} \frac{1}{\epsilon_i} P_\ell(\cos\theta), \tag{1}$$

where $P_\ell(\cos\theta)$ is the Legendre polynomial of order ℓ and ϵ_i is the efficiency for each event, depending on its phase-space location. Structures related to a spin J resonance described by the helicity angle θ, can show up in the Legendre moments of rank up to $l = 2J$, or up to $l = J + J'$ in interferences of J and J' amplitudes. Mass dependence of the Legendre moments can provide hints about resonances present in the data, since their quantum numbers restrict J values. Unfortunately, reflections of decays from the other decay chain(s) can generate mass-dependent variations of the moments at any rank, obscuring the interpretation of the data.

The moment distribution is obtained by weighting each event by a weight $\frac{1}{\epsilon_i} P_\ell(\cos\theta)$. The background contribution in the data is subtracted, and the signal contribution is obtained as the moments distribution of events in the signal region minus the moments distribution of sideband events. The latter is scaled by the ratio of background yields between the signal and the sideband regions. In Fig. 6, we show the Legendre moments vs. $m_{J/\psi\phi}$ using the cosine of helicity angle of $J/\psi\phi$ as the argument of the polynomial. The default model describes the data reasonably well. Improvements over the old Run 1 model are clearly visible in several moments.

In Fig. 7, the Legendre moments vs. $m_{\phi K}$ using the cosine helicity angle of ϕK are shown. The agreement is again reasonable.

The Legendre moments vs $m_{J/\psi K}$ using the cosine helicity angle of $J/\psi K$ are shown in Fig. 8. Improvements with respect to the Run 1 model are obtained.
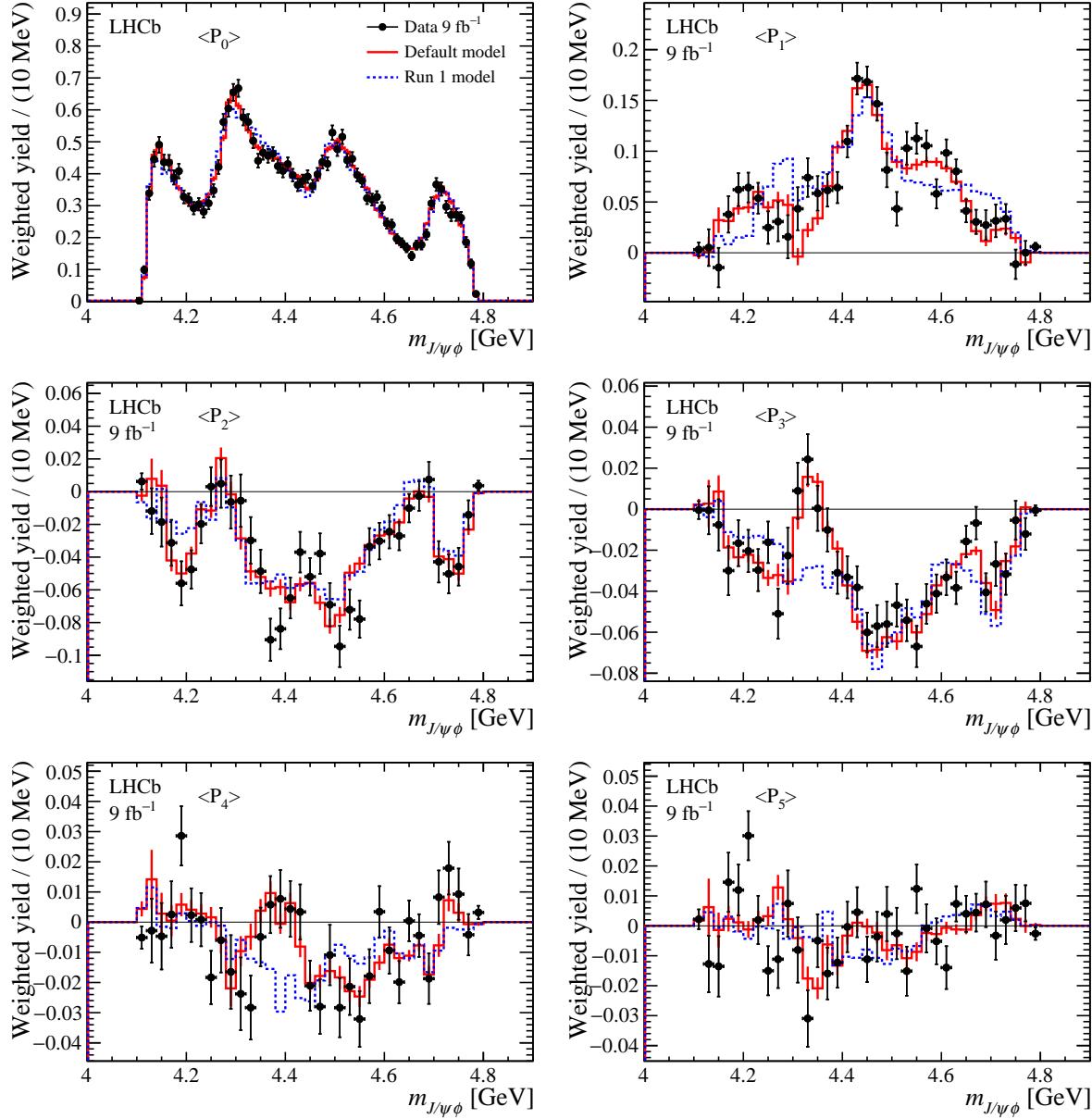
Figure 6: Angular moments of $J/\psi\phi$ helicity angle as a function of $m_{J/\psi\phi}$ compared between the background-subtracted and efficiency-corrected data, PDFs from Run 1 model (blue dashed) and the default model (red solid). The χ^2/nbin for the fit of default model (Run 1 model) are 83(136)/69, 59(117)/35, 48(89)/35, 33(89)/35, 42(81)/35, 55(65)/35 for order from 0 to 5, respectively.
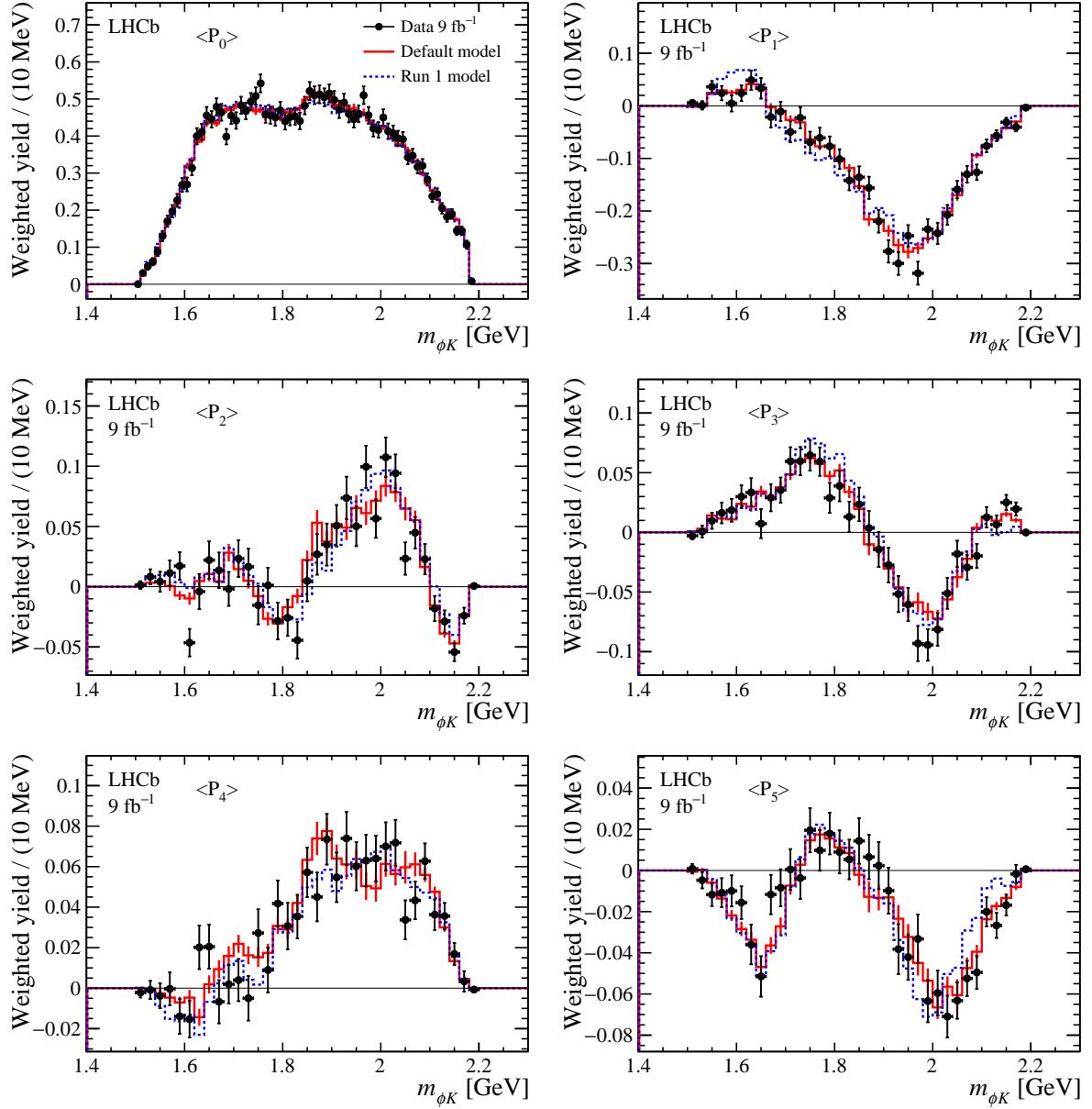
Figure 7: Signal angular moments of ϕK helicity angle as a function of $m_{\phi K}$ compared between the background-subtracted and efficiency-corrected data, PDFs from Run 1 model (blue dashed) and the default model (red solid). The χ^2/nbin for the fit of default model (Run 1 model) are 66(79)/69, 37(86)/35, 49(48)/35, 35(59)/35, 46(44)/35, 36(74)/35 for order from 0 to 5, respectively.
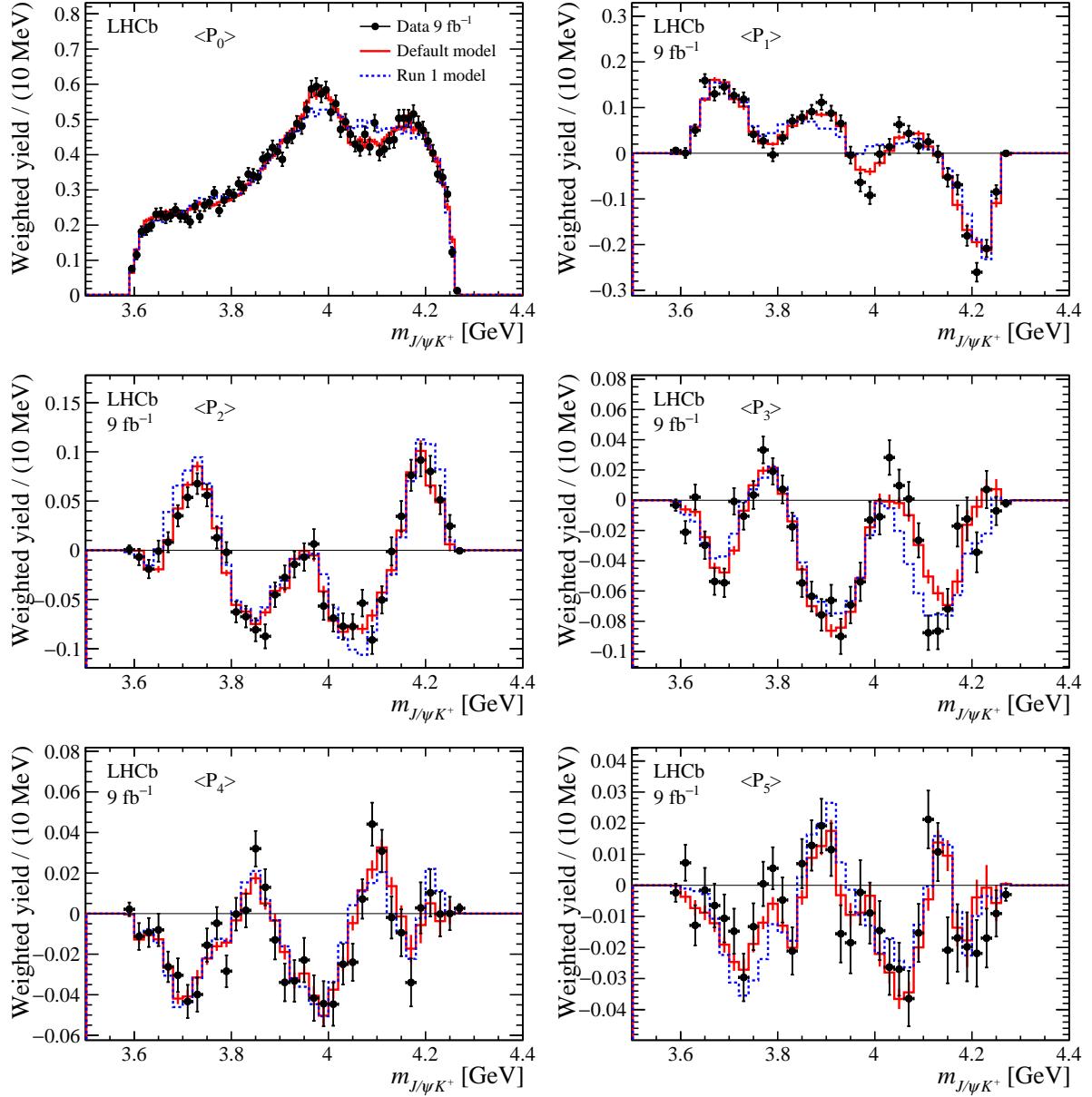
Figure 8: Angular moments of $J/\psi K$ helicity angle as a function of $m_{\phi K}$ compared between the background-subtracted and efficiency-corrected data, PDFs from Run 1 model (blue dashed) and the default model (red solid). The χ^2/nbin for the fit of default model (Run 1 model) are 77(138)/69, 50(108)/35, 30(75)/35, 60(81)/35, 31(41)/35, 44(68)/35 for order from 0 to 5, respectively.

2 Table of systematic uncertainties

The systematic uncertainties for $Z_{cs}(4000)^+$ and $X(4685)$ states are shown in Table 2.

Table 2: Summary of the systematic errors on the parameters of the $Z_{cs}(4000)^+$ and $X(4685)$ states. All numbers for masses and widths are in MeV and fit fractions in %.

Source	$Z(4000)$			$X(4685)$		
	M_0	Γ_0	FF	M_0	Γ_0	FF
Fixed $M_0\&\Gamma_0$	-0.22	-3.60	-0.83	-0.14	2.72	0.25
χ^2_{IP} smearing	0.21	1.01	0.09	-0.53	1.11	0.12
Right sideband	0.01	0.58	0.11	-0.13	1.07	-0.13
Left sideband	-0.30	-1.16	-0.24	-0.09	-2.21	0.09
$\beta = 0.043$	-0.06	-0.00	0.01	0.01	-0.70	-0.09
$\beta = 0.037$	-0.02	0.26	0.02	-0.33	0.21	0.03
L0 Trigger	0.45	0.58	0.19	-0.58	1.12	0.11
PID efficiency	-1.06	-1.82	-0.69	-0.82	-4.42	-0.26
MC size	2.39	9.93	1.54	3.02	7.00	0.65
ϕ window	-4.71	-23.91	-2.75	8.60	-26.60	-1.17
Non ϕ subtraction	-2.87	-18.39	-1.79	12.40	-39.80	-1.80
Poly NR	-4.24	-16.36	-2.56	4.26	-22.07	-1.28
X NR(1^+)	1.49	-21.25	-2.53	-15.72	35.54	3.84
X NR(2^+)	2.16	3.09	1.26	1.88	-6.87	-0.03
BW d=1.5	-0.29	-5.27	-0.58	0.29	1.55	2.14
BW d=4.5	0.08	1.81	0.04	0.06	-3.53	-1.06
L	2.75	-3.19	-1.18	2.45	-24.33	-1.48
$X(4140)$ Flatté	0.52	-2.80	-0.45	-3.77	15.14	1.37
Extended model	-2.35	-6.66	-1.16	-3.61	-6.53	-0.94
Additional X	-0.68	2.07	0.30	0.74	-3.11	-0.18
1^- Z	-14.00	-21.09	-3.46	-9.41	-5.60	-1.52
K^* BW	0.08	-0.66	-0.32	-0.06	-8.09	-0.82
K-Matrix	-3.75	-20.80	-2.85	4.10	-11.95	-0.06
$Z_{cs}(4000)$ Flatté	0.18		2.83	-0.85	2.79	0.18
Background model	0.10	-0.32	-0.12	-1.04	-1.72	-0.15
Total	$(-14.26 ,$ $+3.85)$	$(-26.26,$ $+26.26)$	$(-3.43,$ $+3.41)$	$(-16.05,$ $+12.82)$	$(-40.85,$ $+36.72)$	$(-1.96,$ $+3.92)$

3 Angular distributions

The angular distributions in the ϕK decay chain are shown in Fig. 9, with fit projections overlaid.
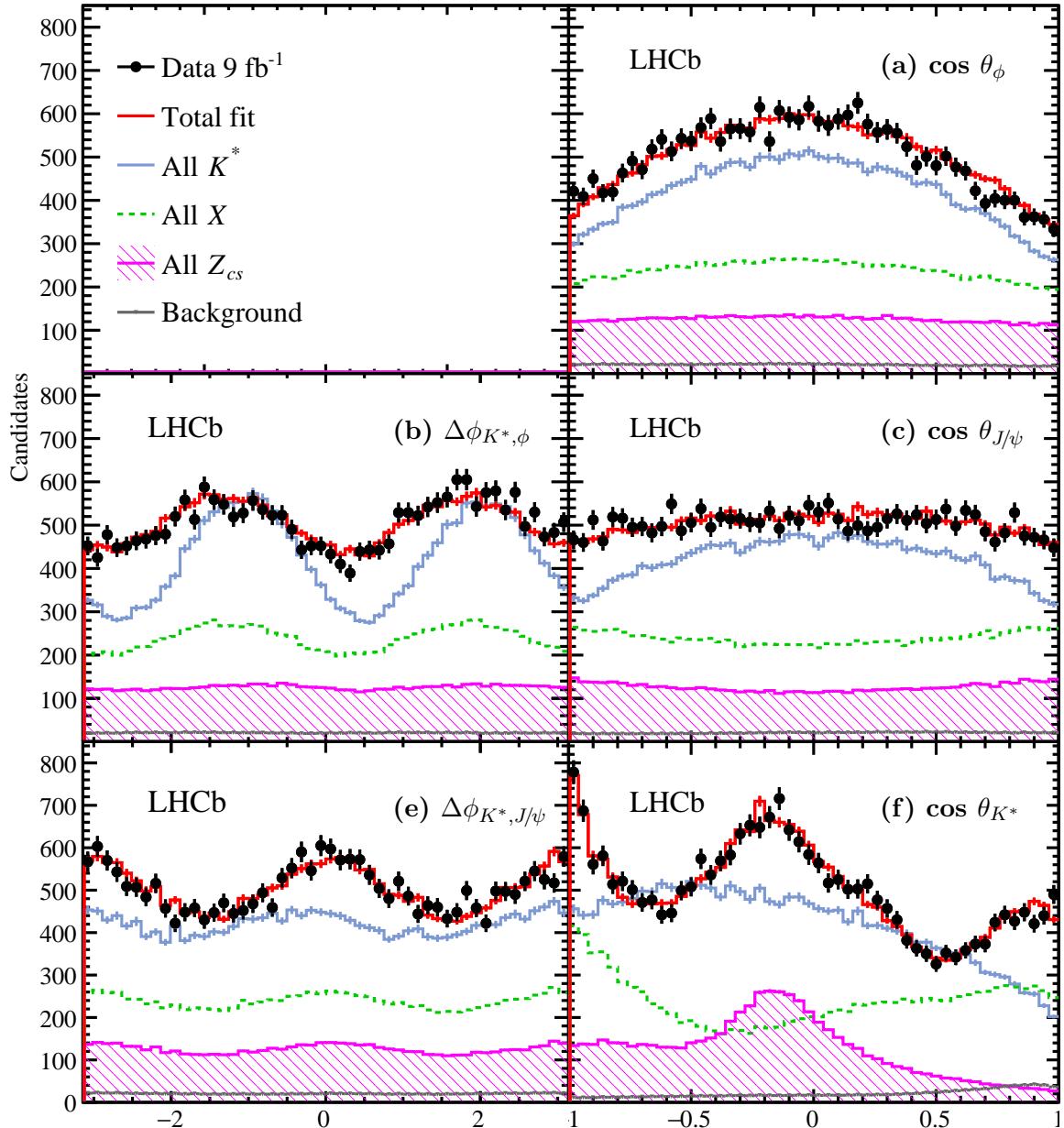
Figure 9: Fit projections of angles in the ϕK decay chain.

4 Individual plots of Figure 3
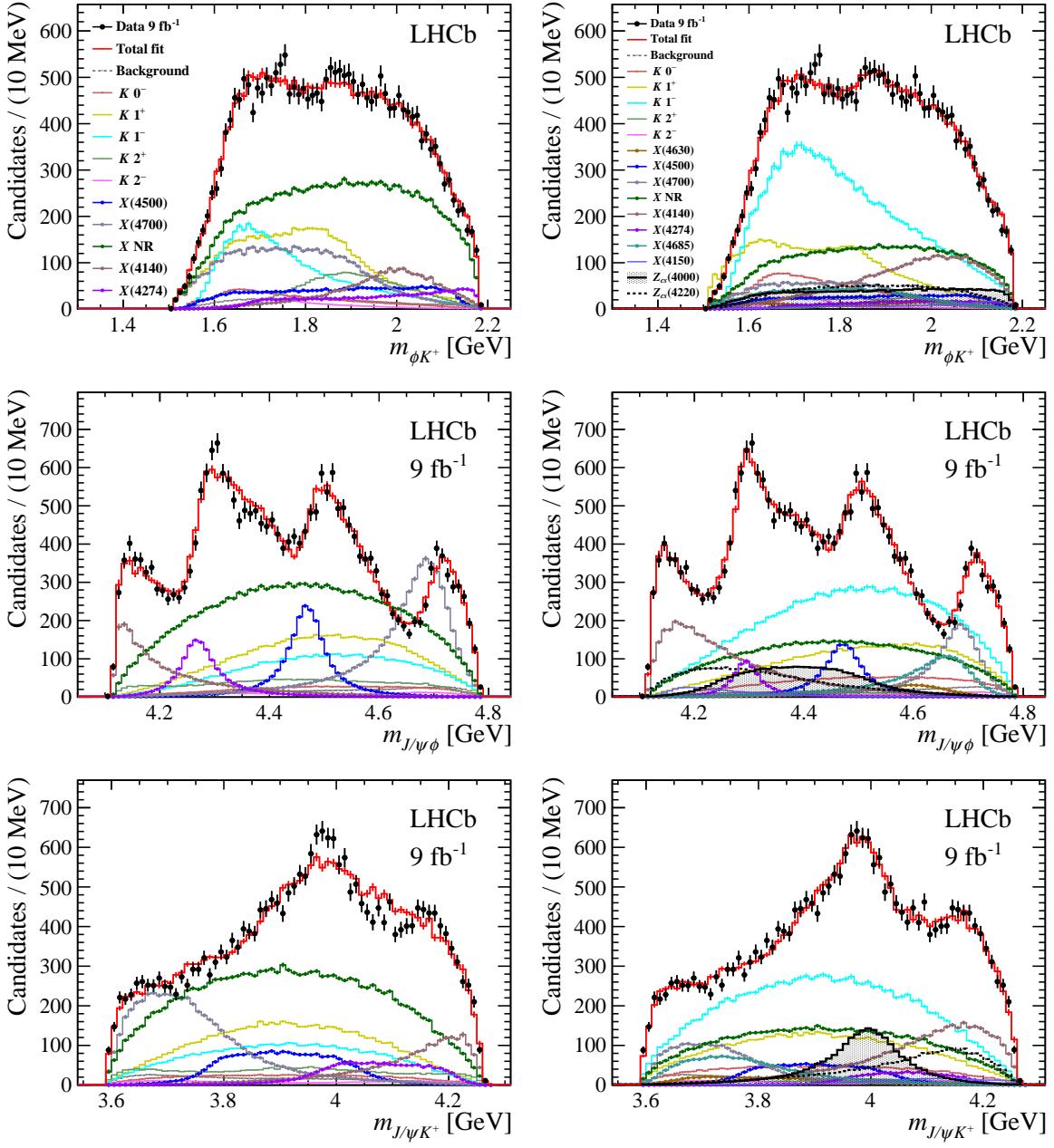
Figure 10: Individual plots of Figure 3, which is merged into one plot in order to save space. The projects in Run 1 model are shown in left, while the default model in right.

5 Run 1 and Run 2 comparison
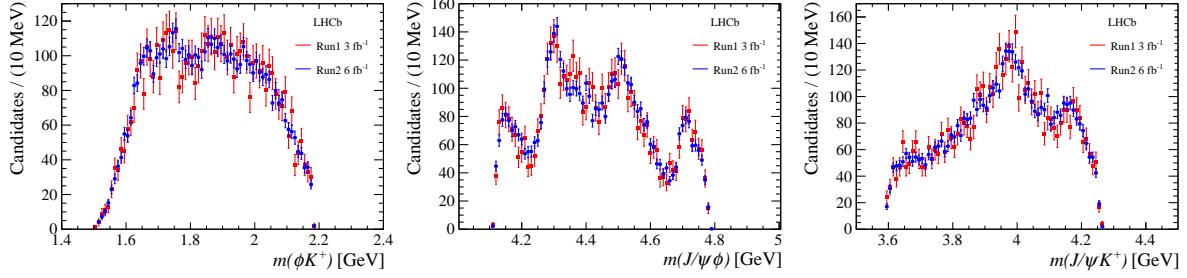
Figure 11: Distributions of (left) ϕK^+, (middle) $J/\psi\phi$ and (right) $J/\psi K^+$ invariant masses for the $B^+ \to J/\psi\phi K^+$ candidates compared between Run1 and Run2 samples. The Run 2 sample is scaled to the same area as that in the Run 1.

LHCb collaboration

R. Aaij[32], C. Abellán Beteta[50], T. Ackernley[60], B. Adeva[46], M. Adinolfi[54], H. Afsharnia[9],
C.A. Aidala[85], S. Aiola[25], Z. Ajaltouni[9], S. Akar[65], J. Albrecht[15], F. Alessio[48], M. Alexander[59],
A. Alfonso Albero[45], Z. Aliouche[62], G. Alkhazov[38], P. Alvarez Cartelle[55], S. Amato[2],
Y. Amhis[11], L. An[48], L. Anderlini[22], A. Andreianov[38], M. Andreotti[21], F. Archilli[17],
A. Artamonov[44], M. Artuso[68], K. Arzymatov[42], E. Aslanides[10], M. Atzeni[50], B. Audurier[12],
S. Bachmann[17], M. Bachmayer[49], J.J. Back[56], S. Baker[61], P. Baladron Rodriguez[46],
V. Balagura[12], W. Baldini[21,48], J. Baptista Leite[1], R.J. Barlow[62], S. Barsuk[11], W. Barter[61],
M. Bartolini[24], F. Baryshnikov[82], J.M. Basels[14], G. Bassi[29], B. Batsukh[68], A. Battig[15],
A. Bay[49], M. Becker[15], F. Bedeschi[29], I. Bediaga[1], A. Beiter[68], V. Belavin[42], S. Belin[27],
V. Bellee[49], K. Belous[44], I. Belov[40], I. Belyaev[41], G. Bencivenni[23], E. Ben-Haim[13],
A. Berezhnoy[40], R. Bernet[50], D. Berninghoff[17], H.C. Bernstein[68], C. Bertella[48], A. Bertolin[28],
C. Betancourt[50], F. Betti[20,d], Ia. Bezshyiko[50], S. Bhasin[54], J. Bhom[35], L. Bian[73], M.S. Bieker[15],
S. Bifani[53], P. Billoir[13], M. Birch[61], F.C.R. Bishop[55], A. Bitadze[62], A. Bizzeti[22,k], M. Bjørn[63],
M.P. Blago[48], T. Blake[56], F. Blanc[49], S. Blusk[68], D. Bobulska[59], J.A. Boelhauve[15],
O. Boente Garcia[46], T. Boettcher[64], A. Boldyrev[81], A. Bondar[43], N. Bondar[38,48], S. Borghi[62],
M. Borisyak[42], M. Borsato[17], J.T. Borsuk[35], S.A. Bouchiba[49], T.J.V. Bowcock[60], A. Boyer[48],
C. Bozzi[21], M.J. Bradley[61], S. Braun[66], A. Brea Rodriguez[46], M. Brodski[48], J. Brodzicka[35],
A. Brossa Gonzalo[56], D. Brundu[27], A. Buonaura[50], C. Burr[48], A. Bursche[27], A. Butkevich[39],
J.S. Butter[32], J. Buytaert[48], W. Byczynski[48], S. Cadeddu[27], H. Cai[73], R. Calabrese[21,f],
L. Calefice[15,13], L. Calero Diaz[23], S. Cali[23], R. Calladine[53], M. Calvi[26,j], M. Calvo Gomez[84],
P. Camargo Magalhaes[54], A. Camboni[45,84], P. Campana[23], A.F. Campoverde Quezada[6],
S. Capelli[26,j], L. Capriotti[20,d], A. Carbone[20,d], G. Carboni[31], R. Cardinale[24,h], A. Cardini[27],
I. Carli[4], P. Carniti[26,j], L. Carus[14], K. Carvalho Akiba[32], A. Casais Vidal[46], G. Casse[60],
M. Cattaneo[48], G. Cavallero[48], S. Celani[49], J. Cerasoli[10], A.J. Chadwick[60], M.G. Chapman[54],
M. Charles[13], Ph. Charpentier[48], G. Chatzikonstantinidis[53], C.A. Chavez Barajas[60],
M. Chefdeville[8], C. Chen[3], S. Chen[27], A. Chernov[35], V. Chobanova[46], S. Cholak[49],
M. Chrzaszcz[35], A. Chubykin[38], V. Chulikov[38], P. Ciambrone[23], M.F. Cicala[56], X. Cid Vidal[46],
G. Ciezarek[48], P.E.L. Clarke[58], M. Clemencic[48], H.V. Cliff[55], J. Closier[48], J.L. Cobbledick[62],
V. Coco[48], J.A.B. Coelho[11], J. Cogan[10], E. Cogneras[9], L. Cojocariu[37], P. Collins[48],
T. Colombo[48], L. Congedo[19,c], A. Contu[27], N. Cooke[53], G. Coombs[59], G. Corti[48],
C.M. Costa Sobral[56], B. Couturier[48], D.C. Craik[64], J. Crkovská[67], M. Cruz Torres[1], R. Currie[58],
C.L. Da Silva[67], E. Dall'Occo[15], J. Dalseno[46], C. D'Ambrosio[48], A. Danilina[41], P. d'Argent[48],
A. Davis[62], O. De Aguiar Francisco[62], K. De Bruyn[78], S. De Capua[62], M. De Cian[49],
J.M. De Miranda[1], L. De Paula[2], M. De Serio[19,c], D. De Simone[50], P. De Simone[23],
J.A. de Vries[79], C.T. Dean[67], D. Decamp[8], L. Del Buono[13], B. Delaney[55], H.-P. Dembinski[15],
A. Dendek[34], V. Denysenko[50], D. Derkach[81], O. Deschamps[9], F. Desse[11], F. Dettori[27,e],
B. Dey[73], P. Di Nezza[23], S. Didenko[82], L. Dieste Maronas[46], H. Dijkstra[48], V. Dobishuk[52],
A.M. Donohoe[18], F. Dordei[27], A.C. dos Reis[1], L. Douglas[59], A. Dovbnya[51], A.G. Downes[8],
K. Dreimanis[60], M.W. Dudek[35], L. Dufour[48], V. Duk[77], P. Durante[48], J.M. Durham[67],
D. Dutta[62], M. Dziewiecki[17], A. Dziurda[35], A. Dzyuba[38], S. Easo[57], U. Egede[69], V. Egorychev[41],
S. Eidelman[43,v], S. Eisenhardt[58], S. Ek-In[49], L. Eklund[59,w], S. Ely[68], A. Ene[37], E. Epple[67],
S. Escher[14], J. Eschle[50], S. Esen[32], T. Evans[48], A. Falabella[20], J. Fan[3], Y. Fan[6], B. Fang[73],
S. Farry[60], D. Fazzini[26,j], P. Fedin[41], M. Féo[48], P. Fernandez Declara[48], A. Fernandez Prieto[46],
J.M. Fernandez-tenllado Arribas[45], F. Ferrari[20,d], L. Ferreira Lopes[49], F. Ferreira Rodrigues[2],
S. Ferreres Sole[32], M. Ferrillo[50], M. Ferro-Luzzi[48], S. Filippov[39], R.A. Fini[19], M. Fiorini[21,f],
M. Firlej[34], K.M. Fischer[63], C. Fitzpatrick[62], T. Fiutowski[34], F. Fleuret[12], M. Fontana[13],
F. Fontanelli[24,h], R. Forty[48], V. Franco Lima[60], M. Franco Sevilla[66], M. Frank[48], E. Franzoso[21],
G. Frau[17], C. Frei[48], D.A. Friday[59], J. Fu[25], Q. Fuehring[15], W. Funk[48], E. Gabriel[32],

20

T. Gaintseva[42], A. Gallas Torreira[46], D. Galli[20,d], S. Gambetta[58,48], Y. Gan[3], M. Gandelman[2], P. Gandini[25], Y. Gao[5], M. Garau[27], L.M. Garcia Martin[56], P. Garcia Moreno[45], J. García Pardiñas[26,j], B. Garcia Plana[46], F.A. Garcia Rosales[12], L. Garrido[45], C. Gaspar[48], R.E. Geertsema[32], D. Gerick[17], L.L. Gerken[15], E. Gersabeck[62], M. Gersabeck[62], T. Gershon[56], D. Gerstel[10], Ph. Ghez[8], V. Gibson[55], H.K. Giemza[36], M. Giovannetti[23,p], A. Gioventù[46], P. Gironella Gironell[45], L. Giubega[37], C. Giugliano[21,f,48], K. Gizdov[58], E.L. Gkougkousis[48], V.V. Gligorov[13], C. Göbel[70], E. Golobardes[84], D. Golubkov[41], A. Golutvin[61,82], A. Gomes[1,a], S. Gomez Fernandez[45], F. Goncalves Abrantes[63], M. Goncerz[35], G. Gong[3], P. Gorbounov[41], I.V. Gorelov[40], C. Gotti[26], E. Govorkova[48], J.P. Grabowski[17], R. Graciani Diaz[45], T. Grammatico[13], L.A. Granado Cardoso[48], E. Graugés[45], E. Graverini[49], G. Graziani[22], A. Grecu[37], L.M. Greeven[32], P. Griffith[21,f], L. Grillo[62], S. Gromov[82], B.R. Gruberg Cazon[63], C. Gu[3], M. Guarise[21], P. A. Günther[17], E. Gushchin[39], A. Guth[14], Y. Guz[44,48], T. Gys[48], T. Hadavizadeh[69], G. Haefeli[49], C. Haen[48], J. Haimberger[48], T. Halewood-leagas[60], P.M. Hamilton[66], Q. Han[7], X. Han[17], T.H. Hancock[63], S. Hansmann-Menzemer[17], N. Harnew[63], T. Harrison[60], C. Hasse[48], M. Hatch[48], J. He[6,b], M. Hecker[61], K. Heijhoff[32], K. Heinicke[15], A.M. Hennequin[48], K. Hennessy[60], L. Henry[25,47], J. Heuel[14], A. Hicheur[2], D. Hill[49], M. Hilton[62], S.E. Hollitt[15], J. Hu[17], J. Hu[72], W. Hu[7], W. Huang[6], X. Huang[73], W. Hulsbergen[32], R.J. Hunter[56], M. Hushchyn[81], D. Hutchcroft[60], D. Hynds[32], P. Ibis[15], M. Idzik[34], D. Ilin[38], P. Ilten[65], A. Inglessi[38], A. Ishteev[82], K. Ivshin[38], R. Jacobsson[48], S. Jakobsen[48], E. Jans[32], B.K. Jashal[47], A. Jawahery[66], V. Jevtic[15], M. Jezabek[35], F. Jiang[3], M. John[63], D. Johnson[48], C.R. Jones[55], T.P. Jones[56], B. Jost[48], N. Jurik[48], S. Kandybei[51], Y. Kang[3], M. Karacson[48], M. Karpov[81], N. Kazeev[81], F. Keizer[55,48], M. Kenzie[56], T. Ketel[33], B. Khanji[15], A. Kharisova[83], S. Kholodenko[44], K.E. Kim[68], T. Kirn[14], V.S. Kirsebom[49], O. Kitouni[64], S. Klaver[32], K. Klimaszewski[36], S. Koliiev[52], A. Kondybayeva[82], A. Konoplyannikov[41], P. Kopciewicz[34], R. Kopecna[17], P. Koppenburg[32], M. Korolev[40], I. Kostiuk[32,52], O. Kot[52], S. Kotriakhova[38,30], P. Kravchenko[38], L. Kravchuk[39], R.D. Krawczyk[48], M. Kreps[56], F. Kress[61], S. Kretzschmar[14], P. Krokovny[43,v], W. Krupa[34], W. Krzemien[36], W. Kucewicz[35,t], M. Kucharczyk[35], V. Kudryavtsev[43,v], H.S. Kuindersma[32], G.J. Kunde[67], T. Kvaratskheliya[41], D. Lacarrere[48], G. Lafferty[62], A. Lai[27], A. Lampis[27], D. Lancierini[50], J.J. Lane[62], R. Lane[54], G. Lanfranchi[23], C. Langenbruch[14], J. Langer[15], O. Lantwin[50,82], T. Latham[56], F. Lazzari[29,q], R. Le Gac[10], S.H. Lee[85], R. Lefèvre[9], A. Leflat[40], S. Legotin[82], O. Leroy[10], T. Lesiak[35], B. Leverington[17], H. Li[72], L. Li[63], P. Li[17], Y. Li[4], Y. Li[4], Z. Li[68], X. Liang[68], T. Lin[61], R. Lindner[48], V. Lisovskyi[15], R. Litvinov[27], G. Liu[72], H. Liu[6], S. Liu[4], X. Liu[3], A. Loi[27], J. Lomba Castro[46], I. Longstaff[59], J.H. Lopes[2], G.H. Lovell[55], Y. Lu[4], D. Lucchesi[28,l], S. Luchuk[39], M. Lucio Martinez[32], V. Lukashenko[32], Y. Luo[3], A. Lupato[62], E. Luppi[21,f], O. Lupton[56], A. Lusiani[29,m], X. Lyu[6], L. Ma[4], S. Maccolini[20,d], F. Machefert[11], F. Maciuc[37], V. Macko[49], P. Mackowiak[15], S. Maddrell-Mander[54], O. Madejczyk[34], L.R. Madhan Mohan[54], O. Maev[38], A. Maevskiy[81], D. Maisuzenko[38], M.W. Majewski[34], J.J. Malczewski[35], S. Malde[63], B. Malecki[48], A. Malinin[80], T. Maltsev[43,v], H. Malygina[17], G. Manca[27,e], G. Mancinelli[10], R. Manera Escalero[45], D. Manuzzi[20,d], D. Marangotto[25,i], J. Maratas[9,s], J.F. Marchand[8], U. Marconi[20], S. Mariani[22,g,48], C. Marin Benito[11], M. Marinangeli[49], P. Marino[49,m], J. Marks[17], P.J. Marshall[60], G. Martellotti[30], L. Martinazzoli[48,j], M. Martinelli[26,j], D. Martinez Santos[46], F. Martinez Vidal[47], A. Massafferri[1], M. Materok[14], R. Matev[48], A. Mathad[50], Z. Mathe[48], V. Matiunin[41], C. Matteuzzi[26], K.R. Mattioli[85], A. Mauri[32], E. Maurice[12], J. Mauricio[45], M. Mazurek[36], M. McCann[61], L. Mcconnell[18], T.H. Mcgrath[62], A. McNab[62], R. McNulty[18], J.V. Mead[60], B. Meadows[65], C. Meaux[10], G. Meier[15], N. Meinert[76], D. Melnychuk[36], S. Meloni[26,j], M. Merk[32,79], A. Merli[25], L. Meyer Garcia[2], M. Mikhasenko[48], D.A. Milanes[74], E. Millard[56], M. Milovanovic[48], M.-N. Minard[8], L. Minzoni[21,f], S.E. Mitchell[58], B. Mitreska[62], D.S. Mitzel[48], A. Mödden [15], R.A. Mohammed[63], R.D. Moise[61], T. Mombächer[15], I.A. Monroy[74], S. Monteil[9], M. Morandin[28], G. Morello[23], M.J. Morello[29,m], J. Moron[34],

A.B. Morris[75], A.G. Morris[56], R. Mountain[68], H. Mu[3], F. Muheim[58,48], M. Mukherjee[7],
M. Mulder[48], D. Müller[48], K. Müller[50], C.H. Murphy[63], D. Murray[62], P. Muzzetto[27,48],
P. Naik[54], T. Nakada[49], R. Nandakumar[57], T. Nanut[49], I. Nasteva[2], M. Needham[58], I. Neri[21],
N. Neri[25,i], S. Neubert[75], N. Neufeld[48], R. Newcombe[61], T.D. Nguyen[49], C. Nguyen-Mau[49,x],
E.M. Niel[11], S. Nieswand[14], N. Nikitin[40], N.S. Nolte[48], C. Nunez[85], A. Oblakowska-Mucha[34],
V. Obraztsov[44], D.P. O'Hanlon[54], R. Oldeman[27,e], M.E. Olivares[68], C.J.G. Onderwater[78],
A. Ossowska[35], J.M. Otalora Goicochea[2], T. Ovsiannikova[41], P. Owen[50], A. Oyanguren[47],
B. Pagare[56], P.R. Pais[48], T. Pajero[29,m,48], A. Palano[19], M. Palutan[23], Y. Pan[62], G. Panshin[83],
A. Papanestis[57], M. Pappagallo[19,c], L.L. Pappalardo[21,f], C. Pappenheimer[65], W. Parker[66],
C. Parkes[62], C.J. Parkinson[46], B. Passalacqua[21], G. Passaleva[22], A. Pastore[19], M. Patel[61],
C. Patrignani[20,d], C.J. Pawley[79], A. Pearce[48], A. Pellegrino[32], M. Pepe Altarelli[48],
S. Perazzini[20], D. Pereima[41], P. Perret[9], K. Petridis[54], A. Petrolini[24,h], A. Petrov[80],
S. Petrucci[58], M. Petruzzo[25], T.T.H. Pham[68], A. Philippov[42], L. Pica[29,n], M. Piccini[77],
B. Pietrzyk[8], G. Pietrzyk[49], M. Pili[63], D. Pinci[30], F. Pisani[48], A. Piucci[17], Resmi P.K[10],
V. Placinta[37], J. Plews[53], M. Plo Casasus[46], F. Polci[13], M. Poli Lener[23], M. Poliakova[68],
A. Poluektov[10], N. Polukhina[82,u], I. Polyakov[68], E. Polycarpo[2], G.J. Pomery[54], S. Ponce[48],
D. Popov[6,48], S. Popov[42], S. Poslavskii[44], K. Prasanth[35], L. Promberger[48], C. Prouve[46],
V. Pugatch[52], H. Pullen[63], G. Punzi[29,n], W. Qian[6], J. Qin[6], R. Quagliani[13], B. Quintana[8],
N.V. Raab[18], R.I. Rabadan Trejo[10], B. Rachwal[34], J.H. Rademacker[54], M. Rama[29],
M. Ramos Pernas[56], M.S. Rangel[2], F. Ratnikov[42,81], G. Raven[33], M. Reboud[8], F. Redi[49],
F. Reiss[13], C. Remon Alepuz[47], Z. Ren[3], V. Renaudin[63], R. Ribatti[29], S. Ricciardi[57],
K. Rinnert[60], P. Robbe[11], A. Robert[13], G. Robertson[58], A.B. Rodrigues[49], E. Rodrigues[60],
J.A. Rodriguez Lopez[74], A. Rollings[63], P. Roloff[48], V. Romanovskiy[44], M. Romero Lamas[46],
A. Romero Vidal[46], J.D. Roth[85], M. Rotondo[23], M.S. Rudolph[68], T. Ruf[48], J. Ruiz Vidal[47],
A. Ryzhikov[81], J. Ryzka[34], J.J. Saborido Silva[46], N. Sagidova[38], N. Sahoo[56], B. Saitta[27,e],
D. Sanchez Gonzalo[45], C. Sanchez Gras[32], R. Santacesaria[30], C. Santamarina Rios[46],
M. Santimaria[23], E. Santovetti[31,p], D. Saranin[82], G. Sarpis[59], M. Sarpis[75], A. Sarti[30],
C. Satriano[30,o], A. Satta[31], M. Saur[15], D. Savrina[41,40], H. Sazak[9], L.G. Scantlebury Smead[63],
S. Schael[14], M. Schellenberg[15], M. Schiller[59], H. Schindler[48], M. Schmelling[16], B. Schmidt[48],
O. Schneider[49], A. Schopper[48], M. Schubiger[32], S. Schulte[49], M.H. Schune[11], R. Schwemmer[48],
B. Sciascia[23], A. Sciubba[23], S. Sellam[46], A. Semennikov[41], M. Senghi Soares[33], A. Sergi[24,48],
N. Serra[50], L. Sestini[28], A. Seuthe[15], P. Seyfert[48], D.M. Shangase[85], M. Shapkin[44],
I. Shchemerov[82], L. Shchutska[49], T. Shears[60], L. Shekhtman[43,v], Z. Shen[5], V. Shevchenko[80],
E.B. Shields[26,j], E. Shmanin[82], J.D. Shupperd[68], B.G. Siddi[21], R. Silva Coutinho[50], G. Simi[28],
S. Simone[19,c], N. Skidmore[62], T. Skwarnicki[68], M.W. Slater[53], I. Slazyk[21,f], J.C. Smallwood[63],
J.G. Smeaton[55], A. Smetkina[41], E. Smith[14], M. Smith[61], A. Snoch[32], M. Soares[20],
L. Soares Lavra[9], M.D. Sokoloff[65], F.J.P. Soler[59], A. Solovev[38], I. Solovyev[38],
F.L. Souza De Almeida[2], B. Souza De Paula[2], B. Spaan[15], E. Spadaro Norella[25,i], P. Spradlin[59],
F. Stagni[48], M. Stahl[65], S. Stahl[48], P. Stefko[49], O. Steinkamp[50,82], S. Stemmle[17], O. Stenyakin[44],
H. Stevens[15], S. Stone[68], M.E. Stramaglia[49], M. Straticiuc[37], D. Strekalina[82], F. Suljik[63],
J. Sun[27], L. Sun[73], Y. Sun[66], P. Svihra[62], P.N. Swallow[53], K. Swientek[34], A. Szabelski[36],
T. Szumlak[34], M. Szymanski[48], S. Taneja[62], F. Teubert[48], E. Thomas[48], K.A. Thomson[60],
M.J. Tilley[61], V. Tisserand[9], S. T'Jampens[8], M. Tobin[4], S. Tolk[48], L. Tomassetti[21,f],
D. Torres Machado[1], D.Y. Tou[13], M. Traill[59], M.T. Tran[49], E. Trifonova[82], C. Trippl[49],
G. Tuci[29,n], A. Tully[49], N. Tuning[32], A. Ukleja[36], D.J. Unverzagt[17], E. Ursov[82], A. Usachov[32],
A. Ustyuzhanin[42,81], U. Uwer[17], A. Vagner[83], V. Vagnoni[20], A. Valassi[48], G. Valenti[20],
N. Valls Canudas[45], M. van Beuzekom[32], M. Van Dijk[49], E. van Herwijnen[82], C.B. Van Hulse[18],
M. van Veghel[78], R. Vazquez Gomez[46], P. Vazquez Regueiro[46], C. Vázquez Sierra[48], S. Vecchi[21],
J.J. Velthuis[54], M. Veltri[22,r], A. Venkateswaran[68], M. Veronesi[32], M. Vesterinen[56], D. Vieira[65],
M. Vieites Diaz[49], H. Viemann[76], X. Vilasis-Cardona[84], E. Vilella Figueras[60], P. Vincent[13],

G. Vitali[29], A. Vollhardt[50], D. Vom Bruch[10], A. Vorobyev[38], V. Vorobyev[43,v], N. Voropaev[38],
R. Waldi[76], J. Walsh[29], C. Wang[17], J. Wang[5], J. Wang[4], J. Wang[3], J. Wang[73], M. Wang[3],
R. Wang[54], Y. Wang[7], Z. Wang[50], H.M. Wark[60], N.K. Watson[53], S.G. Weber[13], D. Websdale[61],
C. Weisser[64], B.D.C. Westhenry[54], D.J. White[62], M. Whitehead[54], D. Wiedner[15],
G. Wilkinson[63], M. Wilkinson[68], I. Williams[55], M. Williams[64,69], M.R.J. Williams[58],
F.F. Wilson[57], W. Wislicki[36], M. Witek[35], L. Witola[17], G. Wormser[11], S.A. Wotton[55], H. Wu[68],
K. Wyllie[48], Z. Xiang[6], D. Xiao[7], Y. Xie[7], A. Xu[5], J. Xu[6], L. Xu[3], M. Xu[7], Q. Xu[6], Z. Xu[5],
Z. Xu[6], D. Yang[3], Y. Yang[6], Z. Yang[3], Z. Yang[66], Y. Yao[68], L.E. Yeomans[60], H. Yin[7], J. Yu[71],
X. Yuan[68], O. Yushchenko[44], E. Zaffaroni[49], K.A. Zarebski[53], M. Zavertyaev[16,u], M. Zdybal[35],
O. Zenaiev[48], M. Zeng[3], D. Zhang[7], L. Zhang[3], S. Zhang[5], Y. Zhang[5], Y. Zhang[63],
A. Zhelezov[17], Y. Zheng[6], X. Zhou[6], Y. Zhou[6], X. Zhu[3], V. Zhukov[14,40], J.B. Zonneveld[58],
S. Zucchelli[20,d], D. Zuliani[28], G. Zunica[62].

[1] *Centro Brasileiro de Pesquisas Físicas (CBPF), Rio de Janeiro, Brazil*
[2] *Universidade Federal do Rio de Janeiro (UFRJ), Rio de Janeiro, Brazil*
[3] *Center for High Energy Physics, Tsinghua University, Beijing, China*
[4] *Institute Of High Energy Physics (IHEP), Beijing, China*
[5] *School of Physics State Key Laboratory of Nuclear Physics and Technology, Peking University, Beijing, China*
[6] *University of Chinese Academy of Sciences, Beijing, China*
[7] *Institute of Particle Physics, Central China Normal University, Wuhan, Hubei, China*
[8] *Univ. Grenoble Alpes, Univ. Savoie Mont Blanc, CNRS, IN2P3-LAPP, Annecy, France*
[9] *Université Clermont Auvergne, CNRS/IN2P3, LPC, Clermont-Ferrand, France*
[10] *Aix Marseille Univ, CNRS/IN2P3, CPPM, Marseille, France*
[11] *Université Paris-Saclay, CNRS/IN2P3, IJCLab, Orsay, France*
[12] *Laboratoire Leprince-Ringuet, CNRS/IN2P3, Ecole Polytechnique, Institut Polytechnique de Paris, Palaiseau, France*
[13] *LPNHE, Sorbonne Université, Paris Diderot Sorbonne Paris Cité, CNRS/IN2P3, Paris, France*
[14] *I. Physikalisches Institut, RWTH Aachen University, Aachen, Germany*
[15] *Fakultät Physik, Technische Universität Dortmund, Dortmund, Germany*
[16] *Max-Planck-Institut für Kernphysik (MPIK), Heidelberg, Germany*
[17] *Physikalisches Institut, Ruprecht-Karls-Universität Heidelberg, Heidelberg, Germany*
[18] *School of Physics, University College Dublin, Dublin, Ireland*
[19] *INFN Sezione di Bari, Bari, Italy*
[20] *INFN Sezione di Bologna, Bologna, Italy*
[21] *INFN Sezione di Ferrara, Ferrara, Italy*
[22] *INFN Sezione di Firenze, Firenze, Italy*
[23] *INFN Laboratori Nazionali di Frascati, Frascati, Italy*
[24] *INFN Sezione di Genova, Genova, Italy*
[25] *INFN Sezione di Milano, Milano, Italy*
[26] *INFN Sezione di Milano-Bicocca, Milano, Italy*
[27] *INFN Sezione di Cagliari, Monserrato, Italy*
[28] *Universita degli Studi di Padova, Universita e INFN, Padova, Padova, Italy*
[29] *INFN Sezione di Pisa, Pisa, Italy*
[30] *INFN Sezione di Roma La Sapienza, Roma, Italy*
[31] *INFN Sezione di Roma Tor Vergata, Roma, Italy*
[32] *Nikhef National Institute for Subatomic Physics, Amsterdam, Netherlands*
[33] *Nikhef National Institute for Subatomic Physics and VU University Amsterdam, Amsterdam, Netherlands*
[34] *AGH - University of Science and Technology, Faculty of Physics and Applied Computer Science, Kraków, Poland*
[35] *Henryk Niewodniczanski Institute of Nuclear Physics Polish Academy of Sciences, Kraków, Poland*
[36] *National Center for Nuclear Research (NCBJ), Warsaw, Poland*
[37] *Horia Hulubei National Institute of Physics and Nuclear Engineering, Bucharest-Magurele, Romania*
[38] *Petersburg Nuclear Physics Institute NRC Kurchatov Institute (PNPI NRC KI), Gatchina, Russia*

[39] *Institute for Nuclear Research of the Russian Academy of Sciences (INR RAS), Moscow, Russia*

[40] *Institute of Nuclear Physics, Moscow State University (SINP MSU), Moscow, Russia*

[41] *Institute of Theoretical and Experimental Physics NRC Kurchatov Institute (ITEP NRC KI), Moscow, Russia*

[42] *Yandex School of Data Analysis, Moscow, Russia*

[43] *Budker Institute of Nuclear Physics (SB RAS), Novosibirsk, Russia*

[44] *Institute for High Energy Physics NRC Kurchatov Institute (IHEP NRC KI), Protvino, Russia, Protvino, Russia*

[45] *ICCUB, Universitat de Barcelona, Barcelona, Spain*

[46] *Instituto Galego de Física de Altas Enerxías (IGFAE), Universidade de Santiago de Compostela, Santiago de Compostela, Spain*

[47] *Instituto de Fisica Corpuscular, Centro Mixto Universidad de Valencia - CSIC, Valencia, Spain*

[48] *European Organization for Nuclear Research (CERN), Geneva, Switzerland*

[49] *Institute of Physics, Ecole Polytechnique Fédérale de Lausanne (EPFL), Lausanne, Switzerland*

[50] *Physik-Institut, Universität Zürich, Zürich, Switzerland*

[51] *NSC Kharkiv Institute of Physics and Technology (NSC KIPT), Kharkiv, Ukraine*

[52] *Institute for Nuclear Research of the National Academy of Sciences (KINR), Kyiv, Ukraine*

[53] *University of Birmingham, Birmingham, United Kingdom*

[54] *H.H. Wills Physics Laboratory, University of Bristol, Bristol, United Kingdom*

[55] *Cavendish Laboratory, University of Cambridge, Cambridge, United Kingdom*

[56] *Department of Physics, University of Warwick, Coventry, United Kingdom*

[57] *STFC Rutherford Appleton Laboratory, Didcot, United Kingdom*

[58] *School of Physics and Astronomy, University of Edinburgh, Edinburgh, United Kingdom*

[59] *School of Physics and Astronomy, University of Glasgow, Glasgow, United Kingdom*

[60] *Oliver Lodge Laboratory, University of Liverpool, Liverpool, United Kingdom*

[61] *Imperial College London, London, United Kingdom*

[62] *Department of Physics and Astronomy, University of Manchester, Manchester, United Kingdom*

[63] *Department of Physics, University of Oxford, Oxford, United Kingdom*

[64] *Massachusetts Institute of Technology, Cambridge, MA, United States*

[65] *University of Cincinnati, Cincinnati, OH, United States*

[66] *University of Maryland, College Park, MD, United States*

[67] *Los Alamos National Laboratory (LANL), Los Alamos, United States*

[68] *Syracuse University, Syracuse, NY, United States*

[69] *School of Physics and Astronomy, Monash University, Melbourne, Australia, associated to [56]*

[70] *Pontifícia Universidade Católica do Rio de Janeiro (PUC-Rio), Rio de Janeiro, Brazil, associated to [2]*

[71] *Physics and Micro Electronic College, Hunan University, Changsha City, China, associated to [7]*

[72] *Guangdong Provencial Key Laboratory of Nuclear Science, Institute of Quantum Matter, South China Normal University, Guangzhou, China, associated to [3]*

[73] *School of Physics and Technology, Wuhan University, Wuhan, China, associated to [3]*

[74] *Departamento de Fisica , Universidad Nacional de Colombia, Bogota, Colombia, associated to [13]*

[75] *Universität Bonn - Helmholtz-Institut für Strahlen und Kernphysik, Bonn, Germany, associated to [17]*

[76] *Institut für Physik, Universität Rostock, Rostock, Germany, associated to [17]*

[77] *INFN Sezione di Perugia, Perugia, Italy, associated to [21]*

[78] *Van Swinderen Institute, University of Groningen, Groningen, Netherlands, associated to [32]*

[79] *Universiteit Maastricht, Maastricht, Netherlands, associated to [32]*

[80] *National Research Centre Kurchatov Institute, Moscow, Russia, associated to [41]*

[81] *National Research University Higher School of Economics, Moscow, Russia, associated to [42]*

[82] *National University of Science and Technology "MISIS", Moscow, Russia, associated to [41]*

[83] *National Research Tomsk Polytechnic University, Tomsk, Russia, associated to [41]*

[84] *DS4DS, La Salle, Universitat Ramon Llull, Barcelona, Spain, associated to [45]*

[85] *University of Michigan, Ann Arbor, United States, associated to [68]*

[a] *Universidade Federal do Triângulo Mineiro (UFTM), Uberaba-MG, Brazil*

[b] *Hangzhou Institute for Advanced Study, UCAS, Hangzhou, China*

[c] *Università di Bari, Bari, Italy*

[d] *Università di Bologna, Bologna, Italy*

[e] *Università di Cagliari, Cagliari, Italy*

[f] Università di Ferrara, Ferrara, Italy

[g] Università di Firenze, Firenze, Italy

[h] Università di Genova, Genova, Italy

[i] Università degli Studi di Milano, Milano, Italy

[j] Università di Milano Bicocca, Milano, Italy

[k] Università di Modena e Reggio Emilia, Modena, Italy

[l] Università di Padova, Padova, Italy

[m] Scuola Normale Superiore, Pisa, Italy

[n] Università di Pisa, Pisa, Italy

[o] Università della Basilicata, Potenza, Italy

[p] Università di Roma Tor Vergata, Roma, Italy

[q] Università di Siena, Siena, Italy

[r] Università di Urbino, Urbino, Italy

[s] MSU - Iligan Institute of Technology (MSU-IIT), Iligan, Philippines

[t] AGH - University of Science and Technology, Faculty of Computer Science, Electronics and Telecommunications, Kraków, Poland

[u] P.N. Lebedev Physical Institute, Russian Academy of Science (LPI RAS), Moscow, Russia

[v] Novosibirsk State University, Novosibirsk, Russia

[w] Department of Physics and Astronomy, Uppsala University, Uppsala, Sweden

[x] Hanoi University of Science, Hanoi, Vietnam